Mass Spectral Characterization of Lipooligosaccharides from *Haemophilus influenzae* 2019[†]

Sara P. Gaucher,[‡] Mark T. Cancilla,[‡] Nancy J. Phillips,[§] Bradford W. Gibson,[§] and Julie A. Leary*[,‡]

Department of Chemistry, University of California, Berkeley, California 94720, and Department of Pharmaceutical Chemistry, University of California, San Francisco, California 94143

Received May 24, 2000; Revised Manuscript Received August 7, 2000

ABSTRACT: Lipooligosaccharide (LOS) glycoforms from *Haemophilus influenzae* 2019 were profiled using the high-resolution and accurate mass capabilities of Fourier transform ion cyclotron resonance (FT-ICR) mass spectrometry. Sequence and linkage for two previously unknown LOS glycoforms were subsequently obtained through MS^n analyses on FT-ICR and quadrupole ion trap (qIT) instruments. MS^n analysis of negative ion precursors confirmed structural details within the lipid moiety, while CID spectra of sodiated precursor ions provided monosaccharide sequence and linkage for the oligosaccharide portion of the molecule. Results obtained in this study indicate that extensive heterogeneity exists within the oligosaccharide moieties in LOS from *H. influenzae* 2019. More importantly, the data suggest that additional hexose moieties, which are added onto the LOS, are not simple extensions of one particular core structure but rather that structural isomers with different connectivities are present within the heterogeneous mixture.

Nontypable (nonencapsulated) strains of *Haemophilus influenzae* are common commensal organisms in the human upper respiratory tract. The proliferation of nontypable *H. influenzae* in other regions of the respiratory tract, however, leads to a variety of diseases in children and adults, such as acute otitus media, sinusitis, and pneumonia (*1*). Particularly vulnerable to lower respiratory tract infections are the elderly and patients with chronic bronchitis. While the incidence of childhood disease caused by *H. influenzae* type b (bacterial meningitis and other bacteremic diseases) has declined in recent years due to the development of conjugate vaccines, there is no vaccine against nontypable *H. influenzae* (*2*). Since nontypable strains lack a capsular polysaccharide, the development of vaccines against these organisms is less straightforward and requires an alternate strategy (*3*).

Lipooligosaccharides (LOS)[1] are the major component of the outer membrane of nontypable *H. influenzae* and have been associated with microbial virulence and pathogenesis (*4*). *H. influenzae* LOS exist as a mixture of glycoforms which are structurally and antigenically diverse. Immunochemical studies have demonstrated the presence of carbohydrate epitopes which mimic human glycosphingolipid antigens (*5*), suggesting that the pathogen may use LOS structures to evade the host's defense mechanisms. Additionally, many LOS carbohydrate epitopes are involved in rapid-phase variation (*6*), a mechanism by which the pathogen can dramatically alter its LOS population during the course of natural infections. Through this process, LOS species which are minor components in bacterial cultures grown in vitro may actually be expressed abundantly in vivo. Thus, to investigate structure/function relationships for LOS, it is important to understand all of the LOS biosynthetic pathways available to the organism and fully characterize as many LOS glycoforms as possible.

Previously, Phillips et al. (*7*) reported the structural analysis of LOS from *H. influenzae* nontypable strain 2019. They found that the major glycoform was a lactose-containing hexasaccharide ketosidically linked via a single bridging 3-deoxy-D-*manno*-octulosonic acid (Kdo) residue to a lipid A moiety. The structure also contained a heptose trisaccharide core region, two phosphoethanolamine (PEA) residues on the oligosaccharide, and a phosphate group on the 4-position of the Kdo. In addition to this major glycoform, both truncated and extended structures were detected in the mixture as additional components. By mass measurements, some of the minor glycoforms were proposed to contain additional hexoses and *N*-acetylhexosamines.

Since the initial study of the LOS from nontypable *H. influenzae* strain 2019 LOS, we and others have conducted structural studies of *H. influenzae* type b LOS from wild-type (*8*, *9*) and mutant strains (*10*−*14*). Although the type b and nontypable organisms cause different infections and are genetically different, all *H. influenzae* LOS studied to date, including the LOS from a type d strain (*15*), have contained the common heptose trisaccharide core and phosphorylated Kdo moiety (*16*). Recently, an unusual nontypable *H. influenzae* LOS structure was reported (*17*) which contained a fourth heptose residue, identified as D-glycero-D-*manno*-

[†] Funding for this research was provided by National Institutes of Health Grants GM47356 (to J.A.L.) and AI31254 and AI24616 (to B.W.G.).

* To whom correspondence should be addressed: phone, (510) 643-6499; fax, (510) 642-9295; email, leary@socrates.berkeley.edu.

[‡] Department of Chemistry, University of California.

[§] Department of Pharmaceutical Chemistry, University of California.

[1] Abbreviations: CID, collision-induced dissociation; DPLA, diphosphorylated lipid A; FT-ICR, Fourier transform ion cyclotron resonance; Hep, heptose; Hex, hexose; HexNAc, *N*-acetylhexosamine; Kdo, 2-keto-3-deoxyoctulosonic acid; Kdo*, anhydro Kdo; LA, lipid A; LOS, lipooligosaccharide; MS^n, sequential stages of mass spectrometry; NMR, nuclear magnetic resonance; OS, oligosaccharide; PEA, phosphoethanolamine; Phos, phosphate group; qIT, quadrupole ion trap.

10.1021/bi001181k CCC: $19.00
Published on Web 09/15/2000

heptose. This heptose was located outside of the heptose trisaccharide core region on an oligosaccharide branch, a structural feature previously seen only in *Haemophilus ducreyi* LOS (*18*−*21*).

In *H. influenzae* type b LOS, oligosaccharide branches can extend from any one of the three core heptoses. Whether or not similar branching can occur in the LOS from nontypable *H. influenzae* strain 2019 has yet to be established, although some of the minor LOS species present in the nontypable strain are isobaric with LOS found in the type b strains. Thus, as a first step in the analysis of nontypable *H. influenzae* 2019 glycoforms, we sought to determine the branching patterns of two of the higher molecular weight glycoforms and to assess their degree of similarity to the known *H. influenzae* type b LOS structures. Additionally, recent experiments (*22*) have demonstrated the presence of sialic acid in the nontypable *H. influenzae* 2019 LOS fraction, prompting the search for sialylated glycoforms and acceptors for sialic acid among the minor species in the LOS population.

In this report we utilize FT-ICR, quadrupole ion trap mass spectrometry, and alkali metal ion coordination (*23*−*37*) in combination with sequential stages of mass spectrometry (MS^n) in order to isolate and identify two higher order glycoforms which contain an increasing number of hexose moieties (3Hex and 4Hex). These oligomers likely contain, or are the scaffolds for presentation of, biologically interesting terminal epitopes involved in interactions with the host.

EXPERIMENTAL PROCEDURES

Materials. LOS isolated from *H. influenzae* 2019 was obtained from Dr. Michael A. Apicella, Department of Microbiology, University of Iowa. The purified *H. influenzae* "Hex2" OS component was a portion taken from a sample used in a previous analysis (*7*). Acetic acid was purchased from Fisher (Pittsburgh, PA). Acetonitrile (HPLC grade) used for mass spectrometric analyses was purchased from Sigma (St. Louis, MO). Water was generated using a Millipore Milli-Q water purification system. All other reagents and solvents used were of reagent grade.

O-Deacylation of LOS. The *H. influenzae* 2019 LOS sample was O-deacylated as previously described (*7*).

Dephosphorylation of O-Deacylated LOS. The *H. influenzae* 2019 LOS sample was HF-treated as previously described (*7*).

Isolation of OS from Dephosphorylated O-Deacylated LOS. Oligosaccharides were released from O-deacylated lipid A through a mild acid hydrolysis treatment. Between 20 and 40 μg of the dephosphorylated, O-deacylated LOS mixture was dissolved in 20 μL of 1% acetic acid and heated at 90−100 °C for 1 h. After being cooled to room temperature, the reaction was centrifuged, and a portion of the supernatant was diluted for MS analysis as described below.

Preparation of MS Samples. Stock solutions of the O-deacylated LOS mixture and dephosphorylated O-deacylated LOS mixture were prepared by dissolving the samples in water to obtain a concentration of approximately 2 μg/μL. A 2 μL portion of the stock solution which had been drop dialyzed over water for 30 min using a VS 0.025 μm Millipore disk membrane was then diluted to obtain 50 μL of a 50:50 acetonitrile:water solution for MS analysis. Samples from the in situ acid hydrolysis of dephosphorylated, O-deacylated LOS were prepared for MS analysis by diluting 5 μL of the reaction supernatant to obtain 50 μL of sample solution in 70:30 acetonitrile:water. A 1 μL portion of 0.01−0.001 M NaCl was added to the sample solution if necessary to generate sodiated species.

MS Analysis by FT-ICR. Exact mass measurements were performed on an APEX II Fourier transform ion cyclotron resonance (FT-ICR) mass spectrometer (Bruker Daltonics, Billerica, MA), equipped with a 4.7 or 7 T actively shielded superconducting magnet. Ions were generated with an Analytica microspray source (Analytica, Branford, CT) or a home-built nanospray source using metal-coated μtip pipets obtained from World Precision Instruments (Sarasota, FL). The ions were externally accumulated for 2 s in an rf-only hexapole ion guide before being transferred to the ICR cell for mass analysis. Ions of the desired mass-to-charge ratio[2] were isolated for collision-induced dissociation (CID) by a combination of correlated sweeps and correlated shots controlled using correlated harmonic excitation fields (*38*). Sustained off-resonance excitation (SORI) was applied for CID. A pressure of $\sim 2 \times 10^{-6}$ mbar of argon was introduced into the ultrahigh vacuum region, and the ion of interest was activated for 250 ms with a radio-frequency pulse at 500 Hz above its resonant frequency. Each spectrum is an average of 32−64 transients composed of 256K or 512K data points acquired using a Bruker Daltonics data station operating XMASS version 5.0.6.

MS Analysis by qIT-MS. Mass spectral analyses were performed on a quadrupole ion trap mass analyzer (Finnigan LCQ, Thermoquest, San Jose, CA) fitted with the electrospray ionization (ESI) source. Samples were infused into the instrument at a rate of 0.3−2 μL/min. The needle was held at a potential of 3−5 kV (lower voltage was used in conjunction with lower flow rate). Ions were trapped by applying an rf-only potential to the ring electrode, and the automatic gain control was used to regulate the number of ions in the trap. Ions were isolated for CID with the "isolation width" parameter set to 3−4. CID was performed at a q value of 0.25 by applying a supplementary rf voltage across the endcaps for 30 ms. The voltage was applied at the axial secular frequency of the precursor ion and with an amplitude of 0.5−2.5 V. Spectra represent the average of 20−50 scans as defined by the scan function in the Finnigan Xcalibur software version 1.0.

RESULTS AND DISCUSSION

LOS Glycan Profile. To obtain an overview, or profile, of the LOS glycans expressed on the surface of *H. influenzae* 2019, a mass spectrum of the O-deacylated LOS mixture was recorded in the negative ion mode. The LOS had been previously O-deacylated to make these species more easily ionized. Features of the mass spectrum, shown in Figure 1, include charge state envelopes containing doubly and triply charged LOS species. In addition, there is a prominent ion at m/z 951.4568 (calcd 951.4590) which can be assigned to O-deacylated diphosphorylated lipid A moiety. The major glycoform in this mixture contains a hexasaccharide moiety with the composition Hex_2Hep_3Kdo. Phillips et al. (*7*) have

[2] Values cited throughout the manuscript for mass-to-charge ratios represent the monoisotopic masses of the ions.

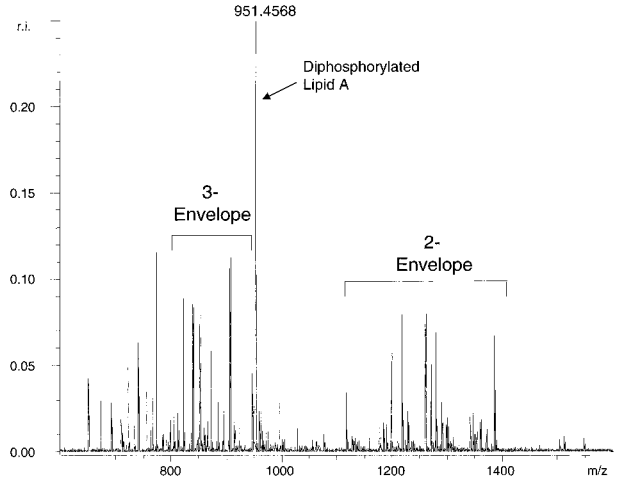

FIGURE 1: FT-ICR negative ion mass spectrum of the O-deacylated lipooligosaccharide mixture isolated from *H. influenzae* 2019.

previously characterized this structure, shown in Figure 2, using a variety of analytical techniques. Several other glycoforms are also present in the mixture, and the proposed compositions for the species contained in the triply charged envelope are listed in Table 1. Singly and doubly charged species contained in the spectrum can be assigned to the same compositions. All structures contain a diphosphorylated lipid A moiety, a Kdo residue, one phosphate group likely to be attached to the Kdo (*7*), and three heptose residues. Structural variations arise from the number of hexose (1−5) and phosphoethanolamine (1−3) residues within the oligosaccharide (OS) moiety. In addition, sodium salts of some of these structures are observed, as well as a species containing *N*-acetylhexosamine (HexNAc) within the OS moiety.

One advantage of using FT-ICR for glycan profiling is the high-resolution mass measurement capability. In such a complex mixture, some components are likely to have the same nominal mass. A resolution of 100 000, routinely achieved by FT-ICR MS, allows one to distinguish between ions which would otherwise be overlapping, as in mass spectra obtained using other instruments. More importantly, the exact mass measurement provided by the FT-ICR can be used to determine elemental composition and thus affords confirmation of the assigned compositions. For example, previous investigations (*7*) of the LOS mixture from strain 2019 had identified components that were hypothesized to contain HexNAc residues within the oligosaccharide moiety. This could not be confirmed at the time, however, due to the fact that a HexNAc residue has the same nominal mass (203 Da) as a phosphate group plus one PEA residue [pyrophosphoethanolamine, a known component of some bacterial LOS (*14*)]. In the current study, accurate mass measurement of the triply charged ion appearing at *m*/*z* 1028.3354 (calcd 1028.3392) confirmed the composition assignment DPLA, Kdo, Phos, 3Hep, 2PEA, 5Hex, 1HexNAc. This assignment has further implications as well: *N*-acetyllactosamine has been identified as one of several acceptors for sialic acid, a major virulence factor, in bacterial LOS. In particular, a glycoform with the same generic composition listed above was identified in *H. influenzae* type b strain A2 in a sialylated form (*8*). Although not observed in the current analysis, sialylated glycoforms could potentially be expressed in strain 2019 under different growth conditions.

As mentioned above, one major glycoform in this mixture has been characterized. The composition of the OS moiety in this species is Hex_2Hep_3Kdo and will be referred to as the "Hex2" species throughout this paper. Additional species contain the same number of heptose and Kdo residues in the OS moiety and either three or four hexose residues. These species are important because it is possible that they could play a role in the virulence of this organism through phase variation (*6*). Of particular relevance is the determination of connectivity of the additional hexose moieties. The question arises as to whether the additional hexose monomers are added onto the existing Hex2 moiety (Figure 2) or whether it is possible that different or additional isomers exist. One goal of this particular study was to obtain structural information including OS sequence and linkage for the "Hex3" and "Hex4" species in the mixture using metal ion coordination—without permethylation or peracetylation—and MS^n. The analyses that follow were performed directly on the glycan mixture; separation of the components was performed in the gas phase through MS^n instead of purifying the compounds by HPLC. In addition, sensitivity was enhanced (*34*), and sample consumption was minimized through the use of micro- and nanoelectrospray ionization.

MS^n Analysis of LOS in the Negative Mode. To simplify subsequent analyses, the mixture was dephosphorylated to remove all phosphate and phosphoethanolamine residues. The resulting mass spectrum contained only one LOS envelope of singly charged species; after treatment, the previously identified Hex2 component appeared at *m*/*z* 1911.8862 (calcd 1911.8805). The other primary components were a "Hex1" structure at *m*/*z* 1749.8081 (calcd 1749.8277) and higher molecular weight components containing 3Hex and 4Hex at *m*/*z* 2073.9262 (calcd 2073.9333) and *m*/*z* 2235.9517 (calcd 2235.9861), respectively. The latter two components were selected for further characterization in order to determine how such structures are constructed, especially in relation to the known Hex2 oligosaccharide.

The first LOS species selected for structural characterization contained the Hex_3Hep_3Kdo OS moiety and appeared at *m*/*z* 2073.9262 in the negative ion mode. An MS^2 analysis was performed on this ion in order to glean as much preliminary information as possible about this LOS component. Surprisingly, under these conditions, very little fragmentation of the OS moiety occurred; the major product ions arose from cleavage of the lipid. In fact, the MS^2 spectrum contained only two major product ions: *m*/*z* 1788.73 and *m*/*z* 1728.71, corresponding to losses of $C_{16}O_3NH_{31}$ and $C_{18}O_5NH_{35}$, respectively (data not shown). These cleavages were assigned to $^{0,2}A$ and $^{0,4}A$ cleavages (*39*) of the first glucosamine residue in the lipid moiety. As diagrammed in Figure 3, these data indicate a 1,6 linkage for this residue.

Further MS analysis of *m*/*z* 1788.73 (MS^3 *m*/*z* 2073.92 → 1788.73 →) yields similar cross-ring cleavage and linkage information for the second glucosamine residue in the lipid and the Kdo residue in the OS moiety. This MS^3 spectrum is shown in Figure 3 along with a diagram of cross-ring cleavage assignments. Product ions appear at *m*/*z* 1401.37 and 1341.43, which correspond to the $^{0,2}A$ and $^{0,4}A$ cleavages, respectively, of the second glucosamine residue, indicating another 1,6 linkage as shown in Figure 3. Cross-ring cleavages at *m*/*z* 1191.33 and 1121.32 were assigned to $^{0,4}A$ and $^{2,4}A$ cleavages within the Kdo moiety, which is consistent

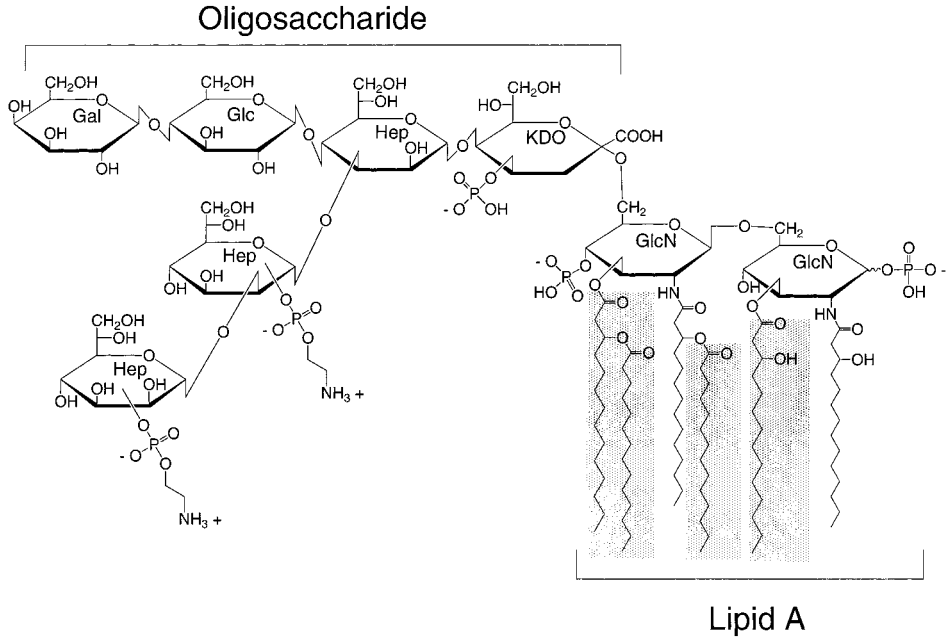

FIGURE 2: Structure of the major lipooligosaccharide component isolated from *H. influenzae* 2019. Shaded boxes indicate the portions of the structure which are eliminated by the O-deacylation procedure.

Table 1: Triply Charged Components Identified from the O-Deacylated LOS Mixture from *H. influenzae* 2019'

obsd *m*/*z* ($z = 3$)	MW		proposed compositions[a,b]
	exptl	theoretical	
744.5805	2233.7415	2233.7286	DPLA KDO Phos 3Hep 2PEA 1Hex
785.5759	2356.7277	2356.7372	DPLA KDO Phos 3Hep 3PEA 1Hex
798.6008[c]	2395.8024	2395.7814	DPLA KDO Phos 3Hep 2PEA 2Hex
811.6073[c]	2434.8219	2434.8257	DPLA KDO Phos 3Hep 1PEA 3Hex
839.5982	2518.7946	2518.7900	DPLA KDO Phos 3Hep 3PEA 2Hex
852.6164	2557.8492	2557.8343	DPLA KDO Phos 3Hep 2PEA 3Hex
865.6284[c]	2596.8852	2596.8786	DPLA KDO Phos 3Hep 1PEA 4Hex
893.6252	2680.8756	2680.8444	DPLA KDO Phos 3Hep 3PEA 3Hex
906.6348	2719.9044	2719.8871	DPLA KDO Phos 3Hep 2PEA 4Hex
947.6344	2842.9032	2842.8956	DPLA KDO Phos 3Hep 3PEA 4Hex
960.6431	2881.9293	2881.9415	DPLA KDO Phos 3Hep 2PEA 5Hex
1028.3354	3085.0062	3085.0193	DPLA KDO Phos 3Hep 2PEA 5Hex 1HexNAc

[a] Observed structures are triply deprotonated. [b] Abbreviations: DPLA, diphosphorylated lipid A; KDO, 2-keto-3-deoxyoctulosonic acid; Phos, phosphate; Hep, heptose; PEA, phosphoethanolamine; Hex, hexose; HexNAc, *N*-acetylhexosamine. [c] These species were also observed as sodium adducts, i.e., $[M + Na - 4H]^{3-}$.

with the Kdo residue linked to the remaining OS moiety through a 1,5 linkage.

Therefore, after three stages of MS in the negative ion mode, confirmation of the monosaccharide linkage within the lipid A moiety was obtained. Additionally, the linkage between the lipid A and OS moiety and the linkage of the Kdo residue to the rest of the OS moiety were identified. These linkages, determined to be 1,6, 1,6, and 1,5 respectively, coincide with previously reported data (*16*) on lipid A and the core structure of OS moieties observed for *H. influenzae* LOS. While these data provided important supporting evidence for the lipid A structure contained in these LOS components, it did not provide sequence or linkage information on the OS portion of the molecule—the true unknown. Therefore, alternative MS experiments were explored, as detailed in the following section.

MS^n Analysis of Sodiated LOS and OS (Positive Ion Mode Detection). (A) Hex3 OS Species. To glean more structural information about the OS moiety, in particular linkage and connectivity, MS^n data were obtained on the sodiated complexes in the positive ion mode. Earlier studies in both our laboratory and that of others have shown that MS^n of alkali (*23*−*37*), alkaline earth (*40*), or transition metal (*41*−*43*) coordinated oligosaccharides provides unambiguous information as to glycosidic linkages in both branched and straight chain oligomers. As previously mentioned, strains of *H. influenzae* appear to share a common OS core consisting of a Kdo linked to three heptose residues as depicted in Figure 4. Thus, one particular goal in analyzing the Hex3 and Hex4 species was to first deduce the connectivity within this core and to determine how the hexoses are linked to the core. This is accomplished via MS^n analysis of the sodiated precursor ions. Additional information as to specific glycosidic linkages is also gained using this methodology.

The FT-ICR positive ion mass spectrum recorded for the LOS mixture is shown in Figure 5. As indicated, there are two main populations of ions: one corresponding to the sodium-cationized LOS series (Hex1 through Hex4) and the other corresponding to the sodium-cationized B-type ions

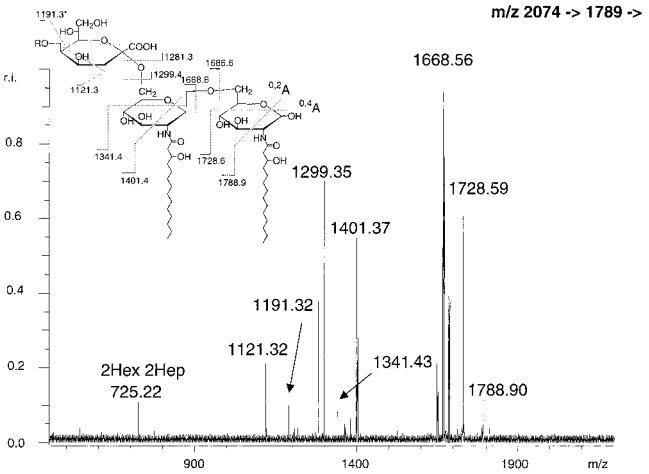

FIGURE 3: FT-ICR negative ion CID spectrum of the dephosphorylated Hex3 LOS species from *H. influenzae* 2019: MS^3 *m/z* 2074 → 1789 →. Inset: Cleavages occurring within the first three residues. R = Hex_3Hep_3. The shaded portion of the structure represents the neutral loss from the MS^2 stage *m/z* 2074 →. The * = cross-ring cleavage concomitant with glycosidic cleavage.

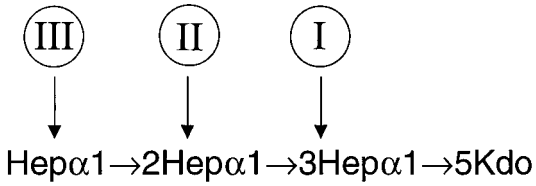

FIGURE 4: Core structure common to *H. influenzae* LOS.

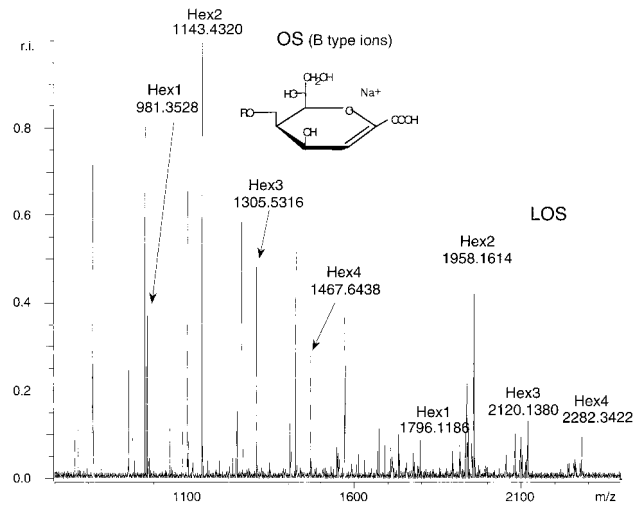

FIGURE 5: FT-ICR positive ion mass spectrum of the dephosphorylated LOS mixture from *H. influenzae* 2019. Labeled ions represent $[M + Na]^+$ species. The B-type ion structure is represented in the inset.

of the OS. The latter envelope was a fortuitous consequence of the electrospray process where the lipid moiety has undergone β elimination from the OS portion of the molecule. These B-type ions were the species chosen for further MS^n analysis.

The FT-ICR MS^2 data obtained from CID of the $[Hex_3Hep_3Kdo + Na]^+$ OS moiety at *m/z* 1305 shown in Figure 6 serves to delineate the monosaccharide connectivity within the Hex3 structure. For example, the ion at *m/z* 599.18 corresponding to $[Hep_3 + Na]^+$ confirms that the three heptoses are sequential while the ion at *m/z* 347.11 corresponds to $[Hex_2 + Na]^+$ and indicates that at least two of the hexoses exist as a dimer. Observed neutral losses narrow the possible branch points within the monosaccharide units: losses of a single hexose (162 Da), heptose (192 Da), and Kdo (220 Da) from the precursor ion at *m/z* 1305.53 indicate that each of these residues must be at a terminating position within the structure. Therefore, no hexose units may be attached at the third heptose as has been observed in other strains (*14*, *15*). These data alone combined with the core known for *H. influenzae* lead to only eight possible structures.[3]

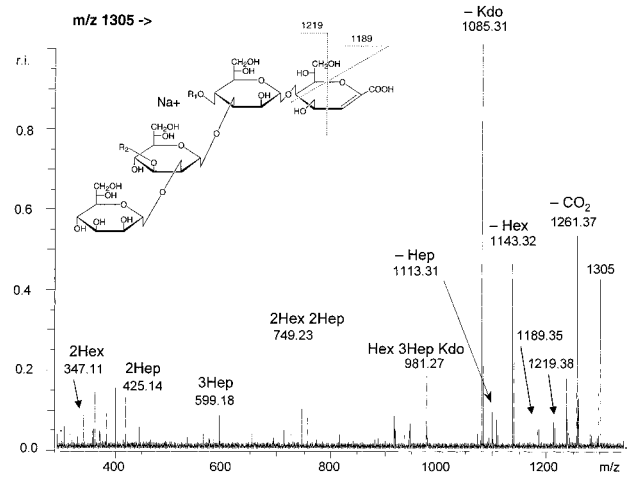

FIGURE 6: FT-ICR positive ion MS^2 spectrum (*m/z* 1305 →) for Hex3 oligosaccharide from *H. influenzae* 2019. Inset: R_1 = Hex, R_2 = Hex_2.

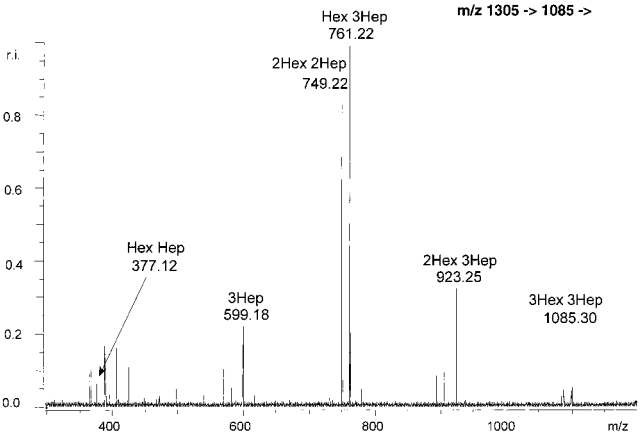

FIGURE 7: FT-ICR positive ion MS^3 spectrum (*m/z* 1305 → 1085 →) for Hex3 oligosaccharide from *H. influenzae* 2019.

Some linkage information is obtained at this MS^n level. There were two cross-ring cleavages observed at *m/z* 1219.38 ($^{2,5}A$) and *m/z* 1189.35 ($^{3,5}A$) within the Kdo moiety as shown in Figure 6. These cleavages complemented the cleavages previously observed in the negative ion mode and thus confirmed the 1,5 linkage between the Kdo and the first heptose residue in the structure.

Because the location and linkage of the Kdo residue are known, the MS^3 spectrum *m/z* 1305.53 → 1085.31 → was recorded as shown in Figure 7, where *m/z* 1085.31 corresponds to loss of the Kdo moiety from the intact Hex3 OS

[3] These structures were calculated using the saccharide topology analysis tool (*45*) and are provided as Supporting Information.

structure. This choice of MS^3 genealogy facilitated obtaining sequence information for the remaining portion of the structure, and closer inspection serves to further narrow the aforementioned list of possible structures. It is unlikely that the structure contains all three hexoses linked together because ions at *m*/*z* 509, corresponding to $[Hex_3 + Na]^+$ and originating from a B-type cleavage, or *m*/*z* 527, corresponding also to $[Hex_3 + Na]^+$ but originating from a C-type cleavage, are missing. (As will be discussed later, MS^n data for the Hex4 species do contain these ions.) More important is the presence of a fairly prominent ion at *m*/*z* 749.23. This ion was prominent in both the MS^2 and MS^3 spectra recorded in the ion trap (data not shown). Such a product ion can only be explained in terms of a single bond cleavage if the precursor ion sequence has one hexose bonded to heptose 1 and two linked to heptose 2 (see Figure 4). In addition, this cleavage was also seen in the negative mode MS^3 spectrum (*m*/*z* 2073.92 → 1788.73 →), where the resulting Hex_2Hep_2 ion appears at *m*/*z* 725.32 (Figure 3). Thus, the connectivity proposed for the Hex3 structure is

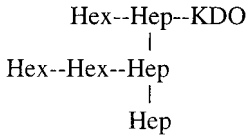

It is important to note that this is not an extension of the structure previously determined for the Hex2 structure. Thus caution should be taken when assuming additive structures based on core configuration.

It remained, however, to ascertain more of the linkages between the monosaccharide units. As mentioned previously, reducing fragments often undergo cross-ring cleavage, which yield linkage position information. Therefore, an MS^4 analysis was performed on the prominent C cleavage at *m*/*z* 749 (*m*/*z* 1305 → 1085 → 749 →). A quadrupole ion trap was used for this particular analysis because of the relative ease of performing MS^n due to efficient retention of the ion of interest during isolation steps and short (seconds) overall experiment time. In this case, the LOS sample was treated with acetic acid prior to analysis to remove the lipid A moiety. This was necessary to circumvent the isobaric interferences occurring between the desired OS B-type ion and sodiated, doubly charged LOS ions. The resulting spectrum is shown in Figure 8 and yields important linkage information about this portion of the structure. First, the ion at *m*/*z* 425 is a heptosylheptose disaccharide and is a C-type ion. In addition, there is an ion at *m*/*z* 275 which represents an $^{0,2}A$ cleavage from this disaccharide. It has been established that $^{0,2}A$ cleavages occur for 1,2- or 1,6-linked disaccharides (*29*, *34*). Second, there is an ion at *m*/*z* 599 which arises from a $C_5H_{10}O_5$ cross-ring cleavage. This 150 Da loss can only occur if the two glycosidic linkages on the reducing end heptose are at adjacent positions on the pyranose ring (see illustration, Figure 8).

Therefore, we propose that the reducing heptose in *m*/*z* 749—i.e., heptose II in the intact structure as shown in Figure 4—is 1,2-linked to the other heptose residue (heptose III in Figure 4) and 1,3-linked to the dihexose branch. This is shown in the inset of Figure 8. In fact, a methylation linkage analysis previously performed on OS fractions obtained from *H. influenzae* 2019 indicated the presence of a 1,2,3-linked

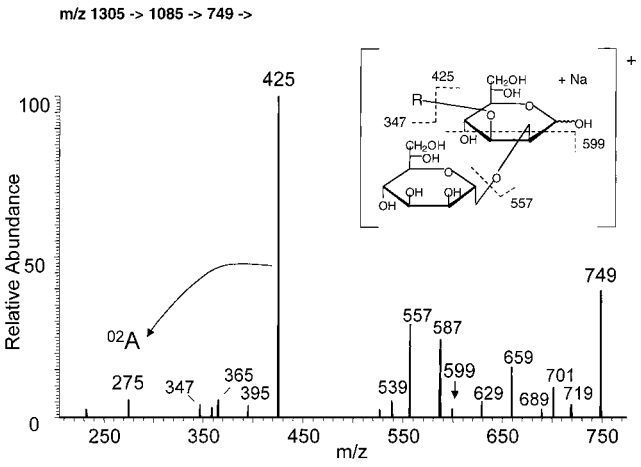

FIGURE 8: Quadrupole ion trap positive ion MS^4 spectrum (*m*/*z* 1305 → 1085 → 749 →) for Hex3 oligosaccharide from *H. influenzae* 2019. Inset: R = Hex_2.

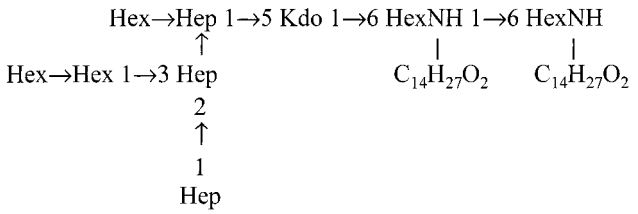

FIGURE 9: Structure proposed for Hex3 lipooligosaccharide contained within the *H. influenzae* 2019 LOS mixture.

heptose (*7*). Taken together, positive and negative ion mode MS^n analysis of the Hex_3Hep_3Kdo LOS species indicates the structure shown in Figure 9.

(B) Hex2 OS Species. As an added check to our assignments, we obtained a purified sample of the isolated Hex2 compound from the LOS mixture. The Hex2 compound was analyzed using the same set of MS^n experiments and methodology as used on Hex3. The assigned structure matched that previously reported (*7*), and its explanation is provided below.

The product ions resulting from MS^2, MS^3, and MS^4 analysis of the $[Hex_2Hep_3Kdo^* + Na]^+$ ion at *m*/*z* 1143 are listed in Table 2. The structure is shown in Figure 2; however, note that only the OS portion of the molecule was present in this sample.[4] As expected, glycosidic cleavages were prevalent and could be used to confirm the monosaccharide sequence. For example, the loss of a hexose (*m*/*z* 981), a heptose (*m*/*z* 951), and the Kdo moiety (*m*/*z* 923) from the precursor ion indicated that at least one hexose, heptose, and the Kdo must be in "terminating" positions. The substantial loss of two hexoses suggested that the two hexoses were on one branch, as was confirmed by the presence of an ion at *m*/*z* 365, $[Hex_2 + Na]^+$, in the MS^3 spectrum. Likewise an ion at *m*/*z* 599, $[Hep_3 + Na]^+$, indicated that the three heptoses were connected in the original structure.

All of the major product ions observed (>5−10% relative abundance) could be assigned to single bond cleavages of the OS structure in Figure 2. There was a relative lack of

[4] Substituted for Kdo at the reducing end is anhydro Kdo (Kdo*). This is due to an artifact of the acid hydrolysis procedure used to remove the lipid moiety as discussed in ref *7*.

Table 2: Product Ions Observed in the MS^2, MS^3, and MS^4 Spectra for Hex2 Oligosaccharide from *H. influenzae* 2019

product ion *m/z*	% relative abundance	neutral loss	cleavage type[a]
	(a) MS^2 spectrum (*m/z* 1143 →)		
1125	3	H_2O	
1099	1	CO_2	
1081	3	CO_2/H_2O	
981	8	Hex	Y
951	5	Hep	Y
941	2	KDO	C
923	39	KDO	B
819	100	2Hex	Y
627	1	2Hex, Hep	Y, Y
599	3	2Hex, KDO	Y, B
521	1	2Hep, KDO	Z, B
	(b) MS^3 spectrum (*m/z* 1143 → 923 →)		
761	15	Hex	Y
749	10	Hep − $2H_2O$	
731	3	Hep	Y
713	2	Hep	Z
599	6	2Hex	Y
581	4	2Hex	Z
539	2	2Hep	B
521	81	2Hep	Z
461	2	unknown	
425	28	2Hex, Hep	C
407	2	2Hex, Hep	B
365	4	3Hep	C
347	2	3Hep	B
	(c) MS^4 spectrum (*m/z* 1143 → 923 → 365 →)		
347	41	H_2O	
305	100	$C_2H_4O_2$	$^{0,4}A$
203	16	Hex	C

[a] See ref *41*.

product ions corresponding to cross-ring cleavage of the oligosaccharide backbone in the MS^2 spectrum. This can be attributed to the absence of a reducing end on the precursor ion which has been shown to initiate such cleavage (*29*, *34*). However, when ions resulting from a C-type cleavage were selected for further MS^n analysis, cross-ring cleavages were present in the spectrum. For example, Table 2c lists the product ions resulting from the MS^4 experiment *m/z* 1143 → 923 → 365. In this particular case, the cross-ring cleavage pattern of the dihexose examined indicated a 1,4-linked disaccharide (*29*, *34*), which corresponds to the correct structure. Therefore, MS^n analysis of C-type ions provides important linkage position information as explained previously for the Hex3 compound.

In summary, CID analysis of the Hex2 OS structure provided monosaccharide sequence, but linkage information only when C ions were first generated. The physical limitations of the quadrupole ion trap prevents low mass ions from appearing in the MS^n spectra (*44*); however, an advantage of this instrument is the ability to quickly perform MS^n analyses. Furthermore, most product ions observed, which were generated through glycosidic cleavage, could be assigned to single bond cleavages from the precursor ion. These basic principles supported our strategy and data interpretation for sequencing and determining linkages of the unknown Hex3 and Hex4 complexes.

(C) Hex4 OS Species. Similar reasoning to that presented above can be used to determine the sequence within the OS moiety corresponding to $[Hex_4Hep_3Kdo + Na]^+$ at *m/z* 1467.64. Again, the sequence of monosaccharide residues

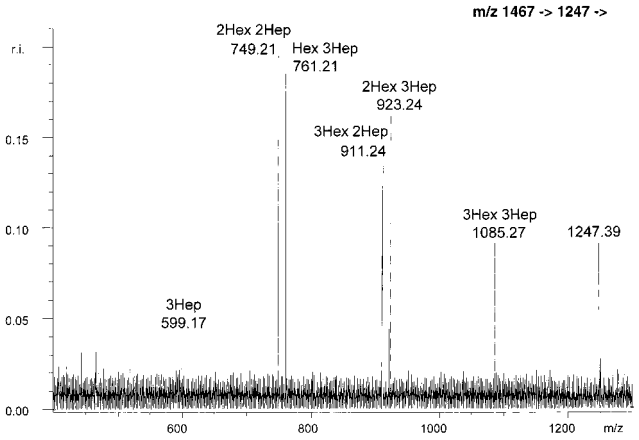

FIGURE 10: FT-ICR positive ion MS^3 spectrum (*m/z* 1467 → 1247 →) for Hex4 oligosaccharide from *H. influenzae* 2019.

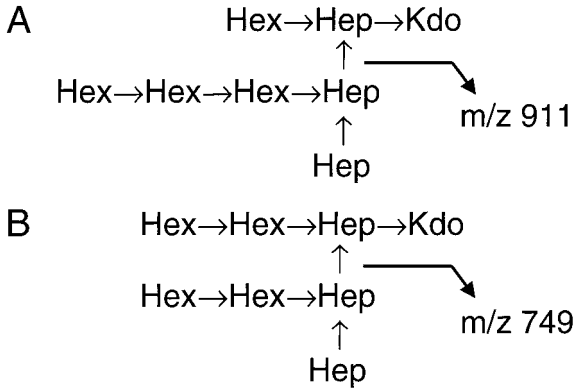

FIGURE 11: (A) Structure proposed for Hex4 oligosaccharide isolated from *H. influenzae* 2019. (B) Alternate structure for this Hex4 oligosaccharide, possibly also present in the mixture.

and branch points was established by the presence of particular ions or observation of particular neutral losses. Product ions appearing at *m/z* 1305.38, 1275.35, and 1247.37 in the MS^2 spectrum (*m/z* 1467.64 →) corresponded to loss of a hexose, heptose, and Kdo residue, respectively, from the precursor ion (data provided as Supporting Information) and again indicated that each of these residue types occupies a terminating position. Therefore, no hexoses are attached to the third heptose. An ion appearing at *m/z* 599.18 was assigned to $[Hep_3 + Na]^+$, which confirmed that the three heptoses must be connected. Similarly, ions at *m/z* 509.15 $[[Hex_3 + Na]^+$ (MS^2 spectrum, Supporting Information)], *m/z* 719.23 $[[Hex_3Hep + Na]^+$ (MS^2 spectrum, Supporting Information)], and *m/z* 911.24 $[[Hex_3Hep_2 + Na]^+$ (Figure 10)] give credence to a structure possessing three sequential hexoses linked to heptose II. However, care must be taken in assigning the structure since more than one isomer may be present in the mixture, as evidenced in the interpretation provided below.

Inspection of the MS^3 spectrum (*m/z* 1467 → 1247 →) in Figure 10 shows the same C-type cleavage (*m/z* 749) present as before, but also extended by one hexose unit (*m/z* 911). Therefore, the proposed sequence for this Hex4 species mimics that for the Hex3 structure with the fourth hexose attached to the hexose chain on the second heptose as shown in Figure 11A.

Given this assignment, it is useful to compare the MS^3 spectrum in Figure 10 with data listed in Table 3 obtained

Table 3: Product Ions Observed in the MS^3 Spectrum (*m*/*z* 1467 → 1247 →) for Hex4 Oligosaccharide from *H. influenzae* 281.25'

product ion *m*/*z*	% relative abundance	neutral loss	cleavage type
1073	8	Hep − $2H_2O$	
923	1	2Hex	Y
905	3	2Hex	Z
749	44	2Hex, Hep	C

in a similar MS^3 experiment for a Hex4 species of known structure. This alternate octasaccharide was isolated from *H. influenzae* strain 281.25 and has been previously purified and characterized (*12*). In this structure, a hexosylhexose disaccharide is attached at both heptose 1 and heptose 2. If the relationship between monosaccharide sequence and dissociation pattern has been correctly deduced, a major pathway of dissociation for this ion is predicted to be a C-type cleavage between the second and third heptose which would appear at *m*/*z* 749. In fact, this is the major product ion in the MS^3 spectrum of this OS structure as shown in Table 3. Furthermore, there is no ion present at *m*/*z* 911 in strain 281.25, which for this structure could only arise through multiple bond cleavages. Therefore, comparison of these spectra supports the structural assignment for the Hex4 species proposed for *H. influenzae* 2019 as shown in Figure 11.

Important to consider is the possibility that there may be more than one isomeric structure for the Hex4 species in *H. influenzae* 2019. Specifically, while the ion at *m*/*z* 911 provides evidence for the presence of the structure proposed in Figure 11A, the fairly abundant ion at *m*/*z* 749 suggests the presence of a structure, described previously, with hexosylhexose disaccharides at heptoses 1 and 2 (Figure 11B). Thus, what cannot be resolved at this time is whether the *m*/*z* 749 ion arises solely from a labile loss of hexose from *m*/*z* 911 or, in addition, an isomer of structure B (Figure 11B) is also present with that of structure A (Figure 11A) in the mixture. Because there is a strong possibility that the Hex4 species may be a mixture of two isomers, further structural elucidation such as linkage position determination was not undertaken at this time. A prerequisite for further MS^n experiments in this case would be chromatographic separation of these isobaric components, a subject of future experiments.

CONCLUSIONS

Connectivity, sequence, and linkage information of previously unknown lipooligosaccharide glycoforms from nontypable *H. influenzae* strain 2019 was obtained using MS^n analysis of both positive and negative ion precursors. In particular, information garnered from CID spectra of various sodiated precursor ions, which included product ions corresponding to extensive cross-ring cleavage of the monomeric units within the oligomer, was crucial for assigning linkage and connectivity. The outlined methodology was also employed in the analysis of two known, previously identified, compounds, thus confirming the previous structural assignment and supporting the proposed method for further analysis of unknown oligosaccharides.

This structural analysis was performed on the LOS mixture directly without prior HPLC separation, and additionally, no derivatization was required. Sample consumption was minimized through use of both nano- and microelectrospray. Both FT-ICR and quadrupole ion trap mass spectrometry were used in this analysis. The high-resolution and accurate mass capabilities of the ICR and the ease of MS^n operation of the ion trap are powerful combinations allowing rapid structural analysis to be performed on a very small amount of sample. In this particular case, high-resolution mass measurements using the FT-ICR allowed for exact mass and thus elemental compositions of the individual LOS to be determined.

Important results obtained in this study indicate that extensive microheterogeneity exists in LOS extracts from *H. influenzae* strain 2019. Data suggest that additional hexose moieties, which are added onto the LOS, are not simple extensions of one particular core structure but rather that structural isomers with different connectivities are present within the heterogeneous mixture. Additional studies are ongoing which will allow for further structural elucidation of other components in the LOS mixture from *H. influenzae* 2019, including possible sialylated compounds.

ACKNOWLEDGMENT

The authors thank Christian Berg from Bruker Daltonics for his assistance in acquiring some of the FT-ICR spectra and Dr. Michael Apicella from the University of Iowa for helpful discussions and for providing lipooligosaccharide samples.

SUPPORTING INFORMATION AVAILABLE

Selected MS^n spectra including tabulated listings of product ions and composition assignments plus calculated structures.[3] This material is available free of charge via the Internet at http://pubs.acs.org.

REFERENCES

1. Murphy, T. F., and Apicella, M. A. (1987) *Rev. Infect. Dis. 9*, 1−15.
2. Kyd, J., and Cripps, A. (1999) *J. Biotechnol. 73*, 103−108.
3. Bernlind, C., and Oscarson, S. (1998) *J. Org. Chem. 63*, 7780−7788.
4. Rao, V. K., Krasan, G. P., Hendrixson, D. R., Dawid, S., and St. Geme, J. W., III (1999) *FEMS Microbiol. Rev. 23*, 99−129.
5. Mandrell, R. E., McLaughlin, R., Abu Kwaik, Y., Lesse, A., Yamasaki, R., Gibson, B., Spinola, S. M., and Apicella, M. A. (1992) *Infect. Immun. 60*, 1322−1328.
6. Weiser, J. N. (1992) *Microb. Pathogen. 13*, 335−342.
7. Phillips, N. J., Apicella, M. A., Griffiss, J. M., and Gibson, B. W. (1992) *Biochemistry 31*, 4515−4526.
8. Phillips, N. J., Apicella, M. A., Griffiss, J. M., and Gibson, B. W. (1993) *Biochemistry 32*, 2003−2012.
9. Masoud, H., Moxon, E. R., Martin, A., Krajcarski, D., and Richards, J. C. (1997) *Biochemistry 36*, 2091−2103.
10. Schweda, E. K. H., Hegedus, O. E., Borrelli, S., Lindberg, A. A., Weiser, J. N., Maskell, D. J., and Moxon, E. R. (1993) *Carbohydr. Res. 246*, 319−330.
11. Schweda, E. K. H., Jansson, P.-E., Moxon, E. R., and Lindberg, A. A. (1995) *Carbohydr. Res. 272*, 213−224.
12. Phillips, N. J., McLaughlin, R., Miller, T. J., Apicella, M. A., and Gibson, B. W. (1996) *Biochemistry 35*, 5937−5947.
13. Risberg, A., Schweda, E. K. H., and Jansson, P.-E. (1997) *Eur. J. Biochem. 243*, 701−707.
14. Risberg, A., Alvelius, G., and Schweda, E. K. H. (1999) *Eur. J. Biochem. 265*, 1067−1074.

15. Risberg, A., Masoud, H., Martin, A., Richards, J. C., Moxon, E. R., and Schweda, E. K. H. (1999) *Eur. J. Biochem. 261*, 171−180.
16. Hood, D. W., Richards, J. C., and Moxon, E. R. (1999) *Biochem. Soc. Trans. 27*, 493−498.
17. Rahman, M. M., Gu, X.-X., Tsai, C.-M., Kolli, V. S. K., and Carlson, R. W. (1999) *Glycobiology 9*, 1371−1380.
18. Melaugh, W., Phillips, N. J., Campagnari, A. A., Karalus, R., and Gibson, B. W. (1992) *J. Biol. Chem. 267*, 13434−13439.
19. Melaugh, W., Phillips, N. J., Campagnari, A. A., Tullius, M. V., and Gibson, B. W. (1994) *Biochemistry 33*, 13070−13078.
20. Schweda, E. K. H., Sundstrom, A. C., Eriksson, L. M., Jonasson, J. A., and Lindberg, A. A. (1994) *J. Biol. Chem. 269*, 12040−12048.
21. Schweda, E. K. H., Jonasson, J. A., and Jansson, P.-E. (1995) *J. Bacteriol. 177*, 5316−5321.
22. M. V. Tullius, unpublished results.
23. Wright, L. G., Cooks, R. G., and Wood, K. V. (1985) *Biomed. Mass Spectrom. 12*, 159−162.
24. Coates, M. L., and Wilkins, C. L. (1987) *Anal. Chem. 59*, 197−200.
25. Lam, Z., Comisarow, M. B., and Dutton, G. G. S. (1988) *Anal. Chem. 60*, 2306−2309.
26. Orlando, R., Buch, C. A., and Fenselau, C. (1990) *Biomed. Environ. Mass Spectrom. 19*, 747−754.
27. Spengler, B., Dolce, J. W., and Cotter, R. J. (1990) *Anal. Chem. 62*, 1731−1737.
28. Zhou, Z., Ogden, S., and Leary, J. A. (1990) *J. Org. Chem. 55*, 5444−5446.
29. Hofmeister, G. E., Zhou, Z., and Leary, J. A. (1991) *J. Am. Chem. Soc. 113*, 5964−5970.
30. Staempfli, A., Zhou, Z., and Leary, J. A. (1992) *J. Org. Chem. 57*, 3590−3594.
31. Dongré, A., and Wysocki, V. H. (1994) *Org. Mass Spectrom. 29*, 700−702.
32. Cancilla, M. T., Penn, S. G., Carroll, J. A., and Lebrilla, C. B. (1996) *J. Am. Chem. Soc. 118*, 6736−6745.
33. Penn, S. G., Cancilla, M. T., and Lebrilla, C. B. (1996) *Anal. Chem. 68*, 2331−2339.
34. Asam, M. R., and Glish, G. L. (1997) *J. Am. Soc. Mass Spectrom. 8*, 987−995.
35. Bahr, U., Pfenniger, A., Karas, M., and Stahl, B. (1997) *Anal. Chem. 69*, 4530−4535.
36. Harvey, D. J., Bateman, R. H., and Green, M. R. (1997) *J. Mass Spectrom. 32*, 167−187.
37. Kovacik, V., Hirsch, J., and Heerma, W. (1997) *Rapid Commun. Mass Spectrom. 11*, 1353−1356.
38. deKoning, L. J., Nibbering, N. M. M., vanOrden, S. L., Laukien, F. H. (1997) *Int. J. Mass Spectrom. Ion Proc. 165*, 209−219.
39. Domon, B., and Costello, C. E. (1988) *Glycoconjugate J. 5*, 397−409.
40. Fura, A., and Leary, J. A. (1993) *Anal. Chem. 65*, 2805.
41. Kohler, M., and Leary, J. A. (1995) *Anal. Chem. 67*, 3501−3508.
42. Sible, E. M., Brimmer, S. P., and Leary, J. A. (1997) *J. Am. Soc. Mass Spectrom. 8*, 32.
43. König, S., and Leary, J. A. (1998) *J. Am. Soc. Mass Spectrom. 9*, 1125−1134.
44. March, R. E. (1997) *J. Mass Spectrom. 32*, 351−369.
45. Gaucher, S. P., Morrow, J., and Leary, J. A. (2000) *Anal. Chem. 72*, 2331−2336.

BI001181K